A dynamic model for assessing soil denitrification in large-scale natural wetlands driven by Earth Observations.

Columba Martínez-Espinosa, Sabine Sauvage, Ahmad Al Bitar, Jose Miguel Sánchez Pérez

A dynamic model for assessing soil denitrification in large-scale natural wetlands driven by Earth observations.

Authors

Columba Martínez-Espinosa[1], Sabine Sauvage[1], Ahmad Al Bitar[2] and José Miguel Sánchez-Pérez[1*].*

Affiliation

[1] Laboratoire Ecologie fonctionnelle et environnement, Université de Toulouse, CNRS, INPT, UPS, Toulouse, France.

[2] Centre d'Etudes Spatiales de la Biosphère, Université de Toulouse, CNES/CNRS/IRD/UPS, Toulouse, France.

*corresponding author

columba.mar.es@gmail.com and jose-miguel.sanchez-perez@cnrs.fr

Abstract

The Wetlands Soil Denitrification Model (WSDM) developed here for natural wetlands, is a physical based model that proposes: (i) the inclusion of soil moisture and temperature from satellite Earth Observations at diurnal temporal resolution, (ii) the distinction of soils under different wetland typologies (i.e., flooded forests, freshwater marshes, brackish wetlands, peatlands, and complex wetlands). Despite uncertainties involved, these two features are key to upscale (nitrification/denitrification dynamics) in natural wetlands at landscape, regional and global scale. In this study, the performance of WSDM was validated with soils of flooded forests and freshwater marshes in the central Amazonian floodplain. WSDM multiannual time series (2012-2019) show that climate anomalies intensify denitrification events. Flooded forests were identified with the highest annual denitrification rates. Annual denitrification and N_2O emissions estimated in this study are in line with previous studies.

Highlights

- A novel large-scale dynamic model for wetlands driven by satellite data is presented.
- Temperature and soil moisture are key to shape denitrification dynamics.
- Earth Observations data are advantageous when no field data is available.

Keywords

Nitrogen cycle, denitrification, wetlands, modelling, SMOS

1. Software and data availability

Name of software: Wetlands Soil Denitrification Model

Description: Wetlands Soil Denitrification Model is a parsimonious process-based model for estimation of nitrogen denitrification fluxes in wetland ecosystems
Developers and contact information: Ahmad Al Bitar ahmad.albitar@cesbio.cnes.fr and Columba Martinez Espinosa columba.mar.es@gmail.com
Contributors: C. Martinez-Espinosa, A. Al Bitar, J. M. Sanchez-Perez, S. Sauvage
Year first available: 2022
Program language: Python
Requirements Python3.4+; Windows, Mac OS X, or Linux; PRMS 3 or newer

- numpy (https://numpy.org/) - Numerical Python library, the fundamental scientific python library.
- matplotlib (https://matplotlib.org/) - 2D plotting library.
- scipy (https://scipy.org/) - scientific python library
- basemap (https://matplotlib.org/basemap)

Program size: 9.6 MB / 4930 lines
Availability
This software is open-source and freely available since 2022 on Framagit https://framagit.org/ahmad.albitar/WSDM. An online documentation to help the user going through WSDM modules is provided https://framagit.org/ahmad.albitar/WSDM/-/blob/master/README.rst

The input databases can be customized according the region of interest. For the global application the recommended databases can be found at:

- Soil characteristics database: https://www.isric.org/explore/wise-databases

Size of archive: 89,3 MB
Access form: free access
Year first available: 2016
Reference
Batjes NH 2016. Harmonised soil property values for broad-scale modelling (WISE30sec) with estimates of global soil carbon stocks. Geoderma 2016(269), 61-68 (http://dx.doi.org/10.1016/j.geoderma.2016.01.034)

- Wetlands distribution and typologies database: https://www.worldwildlife.org/publications/global-lakes-and-wetlands-database-lakes-and-wetlands-grid-level-3

Size of archive: 8.85 MB
Access form: free access
Year first available: 2004
Reference:
Lehner, Bernhard, and Petra Döll. "Development and validation of a global database of lakes, reservoirs and wetlands." Journal of hydrology 296.1-4 (2004): 1-22.

- Brightness temperature and Soil moisture catalogue: https://www.catds.fr/Products/Available-products-from-CPDC

Access form: The CATDS-CEC Ifremer research products are freely available on FTP :
ftp.ifremer.fr user : ext-catds-cecos-ifremer/ password : catds2010
or ftp://ext-catds-cecos-ifremer:catds2010@ftp.ifremer.fr/
Reference:
Al Bitar, A., Mialon, A., Kerr, Y. H., Cabot, F., Richaume, P., Jacquette, E., Quesney, A., Mahmoodi, A., Tarot, S., Parrens, M., Al-Yaari, A., Pellarin, T., Rodriguez-Fernandez, N., and Wigneron, J.-P.: The global SMOS Level 3 daily soil moisture and brightness temperature maps, Earth Syst. Sci. Data, 9, 293–315, https://doi.org/10.5194/essd-9-293-2017, 2017.

2. Introduction

Large scale modelling of biogeochemical cycles to quantify GHG budgets has gained importance over the last century. The increasing rate of CO_2, CH_4 and N_2O in the atmosphere represent a major present and future driver of climate change and global warming (Liu and Greaver, 2009; Pasut et al., 2021). The intensive agricultural practices and the use of N-fertilizers has been identified as the main source of N_2O emissions at the global scale. Current N_2O emission coming from anthropogenic origin are doubling the natural emissions (Tian et al., 2020, 2018, 2019).
In addition, fertilizers are also a major cause of eutrophication of rivers, groundwater and oceans (Smith, 2003). Modelling of nitrogen transfer from terrestrial to aquatic ecosystems (Boyer et al., 2006) is used to quantify nutrient carrying capacity of aquatic ecosystems and resilience (Asaeda et al., 2000; Green et al., 2004).
Wetlands play a key role in the global nitrogen cycle (Adame et al., 2019; Martínez-Espinosa et al., 2021), and they have been identified as large scale denitrification hotspots (Quin et al., 2015; Thorslund et al., 2017) as they carry out complete denitrification pathways reducing NO_3 to N_2 in four stages (Canfield et al., 2010). Quantifying where, when and how much nitrification and denitrification occurs based only on large scale measurements remains a challenge.
The relative yield of the intermediates (N_2O and NO) is a function of the soil moisture, nitrates availability and pH (Chen et al., 2015).
Therefore, models have become essential tools to integrate current knowledge and available data. Denitrification and nitrification pathways are well understood and a number of different approaches have been used to develop N cycling models (Adame et al., 2019; Bakken et al., 2012; Burgin and Groffman, 2012; Groffman and Tiedje, 1988; Tiedje et al., 1989), yet their large scale suitability is still limited.
Wetlands Soil Denitrification Model (hereafter WSDM) was specifically conceived for natural wetlands. It is established as a model with rate-controlling properties that allows denitrification quantification at a large scale, using satellite data. Despite all the uncertainties represented by satellite data, it provides data to produce temporal diurnal resolution multiyear time series and allows access to remote locations all over the globe.
Modelling the mechanisms responsible for terrestrial N_2 emission from natural sources is still limited. Assessment of global terrestrial N_2O emissions from natural sources vary up to a factor 3 and range between 3.3 and 9.0 $TgN.yr^{-1}$ (Ciais et al., 2014). Wetlands N_2O annual

contribution estimation from 1981-2010 to the global budget was 0.97 ±0.7 TgN.yr^{-1} (Tian et al., 2015). Later studies reported that natural soils contribute with 5.6 TgN.yr^{-1} in a range of 4.9-6.5 TgN.yr^{-1}, and inland waters, estuaries and coastal zones contribute with 0.3 TgN.yr^{-1} (0.3-0.4 TgN.yr $^{-1}$) (Tian et al., 2020).

These annual estimates are insightful when comparing biomes, and to identify different wetlands entities and their contribution to the global nitrogen cycle. Yet, this assessment does not explain the role of different inland and coastal natural wetlands (i.e. freshwater marshes, flooded forest, peatlands, mangroves and saltmarshes). In addition, the annual assessment does not show evidence related to the hot moments (seasonality). Investigating inter-annual dynamics of denitrification and their relationship with flooding or drought events is relevant for future climate scenarios, WSDM aims to contribute to filling this gap, investigating denitrification exclusively in natural wetlands, and emphasizing the diversity of these ecosystems with spatialized information.

3. Materials and methods

3.1 Wetlands Soils Denitrification Model

The WSDM was developed specifically for natural wetlands ecosystems where complete denitrification occurs (Adame et al., 2019; Guilhen et al., 2020; Martínez-Espinosa et al., 2021). The WSDM aims to model denitrification process in wetlands soils, influenced by three main physical parameters; soil moisture, temperature and nitrates availability. The WSDM model simplifies denitrification process by forcing available daily spatialized data to enable large scale application. A software was developed to harmonize the different databases and to carry out the simulations. The model is developed in Python programming language, using standard scientific computation and visualisation libraries with an open-source license. The code is developed in functional approach with separate modules for pre-processing, simulation and post-processing. The WSDM model with a brief description is available at https://framagit.org/ahmad.albitar/WSDM/

Model implementation

WSDM needs two kind of spatialized data. On one hand, static datasets, define the wetland typology and extension, and the soil characteristics (i.e. texture, bulk density, organic carbon content). On the other hand, dynamic datasets (soil moisture and soil temperature) will lead the nitrification and denitrification processes. Before running the physical-model, a pre-processing phase is carried out. The user then has to define the Region of Interest (ROI), giving two latitude and two longitude points indicating ROI limits, followed by the starting and end date of the simulation period. Once these criteria are established, simulation is launched. Spatial harmonization of databases is the first step, to have n-dimensional data on a regular grid. Soil characteristics database - WISE30sec (Batjes, 2015) was the reference grid, with a spatial resolution of 30 arcsec (1 km^2), well as Global Lakes and Wetlands Database (GLWD) (1 km^2) (Lehner and Doll, 2004). Brightness soil temperature and root zone soil moisture (Ahmad and Mahmoodi Ali, 2020; Al Bitar et al., 2017) have an original grid of

25km^2, therefore a linear interpolation, using (https://scipy.org/) - scientific python library is compute in every simulation, before running the physical model.

The workflow summary WSDM processes (Figure 1). The physical model has different functions that are explained in the next subsections. The limitation of the approach is detailed in the discussion section.

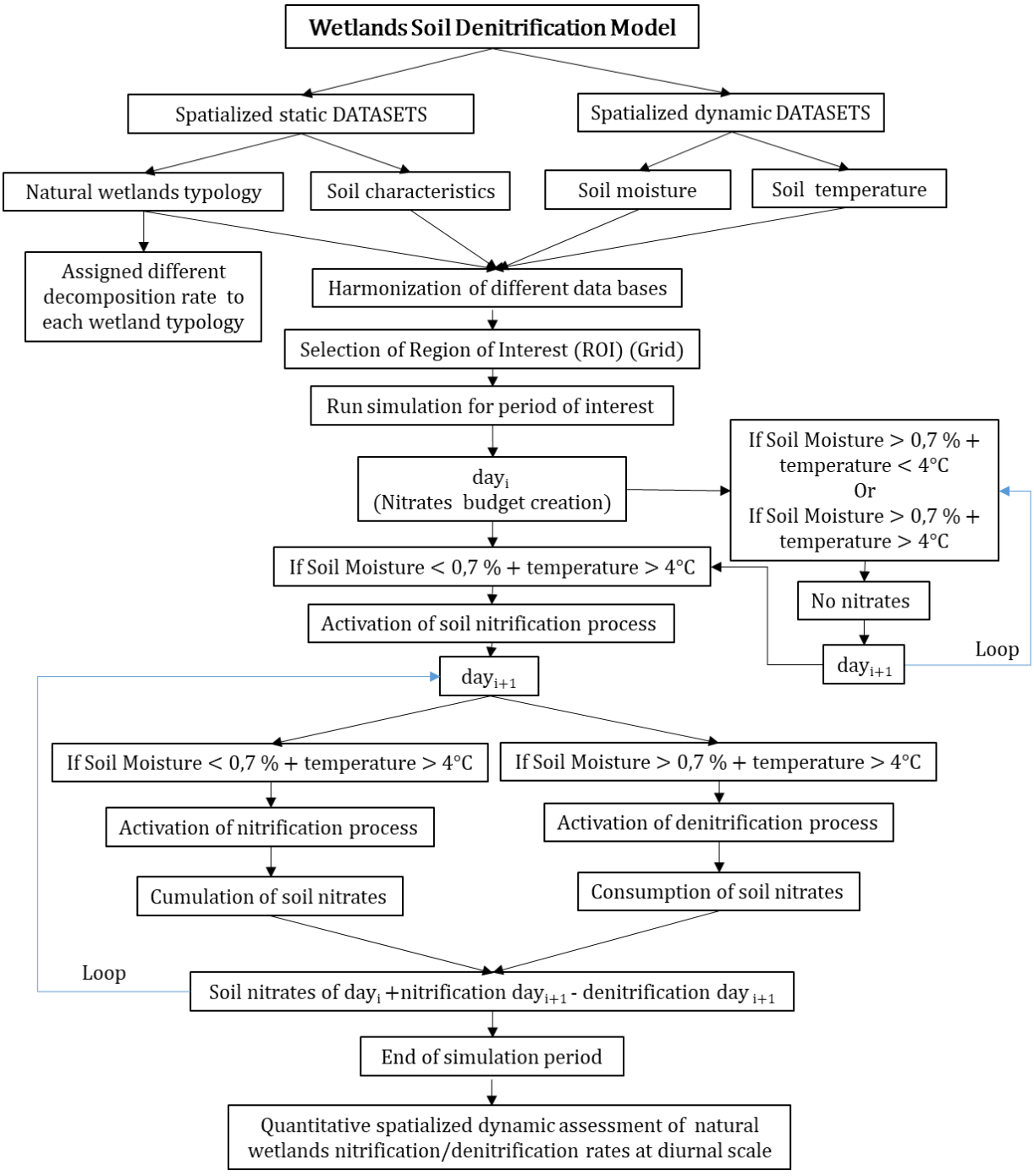

Figure 1. Workflow illustration of the Wetlands Soil Denitrification Model processes flow (black arrows), the blue arrows represent the main two loops of the model. After setting up the model and defining the region of interest the simulation begins with nitrate budget generation in day$_i$. Nitrification will be active if soil moisture is low, if not, no nitrates will be created and no denitrification will be recorded, until that condition changes. Following the workflow, day$_{i+1}$ soil

moisture will define if nitrification or denitrification will occur. This loop will continue happening until the end of the defined simulation period.

NITRIFICATION

In WSDM, nitrification is the first process, as it calculates nitrate production. The first year of the model run is used for stabilization, as the nitrate budget is created at the beginning of the run, therefore a minimum of two years of input data is needed. Nitrification is linked to the stock and evolution of organic matter in the soil, both together define soil fertility. Transported nitrates (i.e. agricultural sources) are not considered in this first version. Nitrates production (Eq. 1) is modelled as follows,

$$NO_{3\,nit} = (N_{org} \cdot k_2 \cdot f_{SM}) \quad \text{Eq. 1}$$

where $NO_{3\,nit}$ corresponds to the nitrates produced by nitrification in the local soil (mgN.kg^{-1}.day^{-1}), given by N_{org} organic nitrogen in soil (mgN.kg^{-1}) (Eq. 2),

$$N_{org} = \frac{C_{org}}{C:N} \quad \text{Eq. 2}$$

where $OrgC$ is the organic carbon in soil (gC.kg^{-1}), and C:N is the ratio of carbon and nitrogen. The destruction of humus by mineralization is variable depending on the soil and the bacteria activity expressed by k_2 coefficient, calculated from the quantity of stable humus in the soil. The rate of mineralization is always higher in warm, humid climates, and varies from 0.5 to 3%. To adjust the k_2 coefficient according to soil texture and temperature (Eq. 3), we used the model proposed for clay soils by Girard et al., (2011),

$$k_2 = \frac{1200}{(C + 200) \cdot (0.3 \cdot [CaCO_3] + 200)} \cdot \rho_b \cdot (0.2 \cdot MAT - 10) \quad \text{Eq. 3}$$

where C and [$CaCO_3$] correspond to the clay (%) and carbonate content (gC.kg^{-1}) respectively, ρ_b is the bulk density (kg.dm^{-3}), and MAT (Mean Annual Temperature) (°C), the coefficients are conversion units factors. The third term f_{SM} represents soil saturation factor (Eq. 4), defined as follows,

$$f_{SM} = \frac{SM_i - SM_{res}}{SM_{sat} - SM_{res}} \quad \text{Eq. 4}$$

$$\text{If } f_{SM} \geq 0.7, NO_{3\,nit} = 0$$

where SM_i, is the soil moisture of day (i) (m^3.m^{-3}), SM_{res} is the lowest soil moisture that allows the reaction to happen, and SM_{sat}, (m^3.m^{-3}). A threshold indicating nitrification can only happen when aerobic conditions are guaranteed. f_{SM} will be used for denitrification (Eq.5), but conditioned inversely.

Denitrification

Denitrification function on WSDM was structured as the NEMIS model (Eq.5) (Hénault and Germon, 2000), adapting the multi-component method (Berner, 1980) where diurnal denitrification (Eq.6) is given by the potential denitrification weighted by three main parameters (i.e. nitrate availability, soil moisture and temperature) adapted as follows,

$$\mathrm{D}i_v = Dp \cdot f_N \cdot f_{SM} \cdot f_T \qquad \text{Eq. 5}$$

Where $\mathrm{D}i_v$ is the denitrification rate in day (i), Dp is the potential denitrification rate in (mole N.dm^{-3}.d^{-1}) calculated from the first order kinetic model (Hunter et al., 1998). This model (Eq. 5), was first adapted for the hyporheic zone by Peyrard et al., (2011). Then modified and tested at larger scale, to calculate the dynamic potential denitrification of flooded areas using satellite data (Guilhen et al., 2020), and subsequently for daily denitrification quantification on floodplains areas in different watershed under tropical, temperate and arctic conditions (Fabre et al., 2020). These advances were key evidence to adopt this denitrification model into the WSDM as follows,

$$Dp = 0.8\,x \cdot \rho_b \frac{1-\varphi}{\varphi} \cdot k_{OC}[OrgC] \qquad \text{Eq. 6}$$

where Dp is the potential denitrification rate in (mole N dm^{-3}.d^{-1}), $0.8x$ represent the stoichiometric proportion of nitrate consumed in denitrification compared to the organic matter used with x = 5, ρ_b is the bulk density (kg.dm^{-3}), φ is the porosity (unitless), k_{oc} (d^{-1}) is organic carbon mineralization constant define for each wetland typology (Table 2), $[OrgC]$ (mole.kg^{-1}) is the organic carbon available in the soil.

Dp is different for each wetland typology, and regulated in function of three main parameters, these three unitless functions range from zero to optimal condition (one). First, f_N represents nitrates soil availability (Eq. 7),

$$f_N = \frac{[NO_{3\,i}^-]}{[NO_{3\,i}^-] + K_{NO_3^-}} \qquad \text{Eq. 7}$$

where f_N depends on the nitrates soil concentration $[NO_{3\,i}^-]$ (mgN.kg^{-1}) and bacteria denitrification capacity, define on the $K_{NO_3^-}$, a half saturation constant for denitrification. This constant was calibrated for wetlands ecosystems in the present study.

Half saturation constant $k_{NO_3^-}$

The half saturation constant is integrated in the denitrification model in a Michaelis Menten type function that limits the denitrification capacity, and is related to nitrates quantity (Peyrard et al., 2011). To adjust this value to wetlands ecosystems (Eq.9), the $k_{NO_3^-}$ constant was calibrated experimentally in the present study (Appendix Experimental Methodology) using the emission results (Appendix Table A.3) as follows,

$$A = \frac{Di}{Dp} \quad \text{Eq. 9}$$

where A is a relation factor between Dp (mgN.kg^{-1}) potential denitrification, and Di (mgN.kg^{-1}) is the control denitrification of the same soil, with no addition of nutritive solution. This factor then is substituted as f_N (Eq. 7) , which allows the $k_{NO_3^-}$ to be calculated as follows,

$$k_{NO_3^-} = \frac{[NO_{3\,i}^-]}{A} - [\,NO_{3\,i}^-] \quad \text{Eq. 10}$$

where $k_{NO_3^-}$(mgN.kg^{-1}) is the half saturation denitrification constant cleared out from the saturation equation 7, using *A*, the unitless relation factor calculated above, as the known f_N. Then the mean $k_{NO_3^-}$ value for all the samples was stablished as the wetlands ecosystems constant (Table 2). The second term f_{SM} represents soil saturation factor, explained above (Eq. 3), conditioned as follows,

$$\text{If } f_{SM} \leq 0.7, NO_{3\,denit} = 0$$

where a threshold indicating denitrification trigger was set at $f_{SM} = 0.7$, as denitrification can only happen when ≥ 70% of water in the soil pores (Bateman and Baggs, 2005). The third term defines temperature impact on denitrification (Eq. 11),

$$f_T = e - \frac{(T_i - T_{opt})^2}{(T_i \cdot T_{opt})} \quad \text{Eq. 11}$$

where T_i is the temperature of the given day and T_{opt} is the optimal temperature for denitrification established as 25°C in natural ecosystems (Billen et al., 2018).
Denitrification Di_v obtained from these equations is volume based (mole N.dm^{-3}.d^{-1}), in order to integrate the result to the WSDM, a conversion from volume to mass (Eq. 12) was applied as follows,

$$Di_m = \frac{Di_v \cdot MmN \cdot 1000}{\rho_b \frac{1-\varphi}{\varphi}} \quad \text{Eq. 12}$$

where, Di_m is expressed in mgN.kg^{-1}.day^{-1}, MmN is the nitrogen molar mass (g), 1000 is the conversion factor g to mg, ρ_b is the bulk density (kg.dm^{-3}), φ is the porosity (unitless).
Nitrates budget in the soil (Eq. 13), is calculated by integrating nitrification and denitrification processes defined as follows,

$$NO_{3_{i+1}}^- = NO_{3_{i-1}}^- + [NO_{3\,i}^-]_{nit} \cdot \delta t - [NO_{3\,i}^-]_{denit} \cdot \delta t \quad \text{Eq. 13}$$

where $NO_{3_{i+1}}^-$(mgN.kg^{-1}) is the nitrates available in the day (*i+1*), given by $NO_{3_{i-1}}^-$(mgN.kg^{-1}), that represents the nitrates that are produced but not yet consumed, $NO_{3_i nit}^-$ (mgN.kg^{-1}) is

the nitrates produced by nitrification on a given day (i) and $NO_{3_i denit}^{-}$ (mgN.kg^{-1}), the nitrates consumed by denitrification on the same day (i) and δt, (day) to denote the time span. This function is activated at the end of each day, before starting the loop. WSDM continues the simulation until the end of the defined period.

Transformation of denitrification rates from mass to area (Eq. 14) was calculated as follows,

$$Denit_{kg.ha} = [NO_{3\,i}^{-}]_{denit} * \rho_b * soil_{act} \quad \text{Eq. 14}$$

where $Denit_{kg.ha}$ is the total denitrification (N_2O-N+N_2-N) estimation in kgN.ha^{-1}.day^{-1}, given by $[NO_{3\,i}^{-}]_{denit}$ (mgN.kg^{-1}) nitrates consumed, ρ_b is the bulk density (kg.dm^{-3}), $soil_{act}$ refers to the active soil layer, here 30 cm was used as a constant depth of the active layer.

N_2O-N_2 RATIO OUTGASSING

N_2O emissions are highly variable in space and time, and there has not been a consensus on a methodology that responds to bottom-up or top-down scales. However, as scale increases, so does the agreement between estimates based on soil surface measurements (bottom-up approach) and estimates derived from changes in atmospheric concentration of N_2O (top-down approach) (Grosso et al., 2008).

The IPCC provides guidelines for estimating regional and global N_2O emissions, which are calculated by multiplying N loading with the indirect emission factors (EF) (IPCC, 1996). The indirect N_2O emission factor associated with N leaching and runoff (EF_5: kg N_2O-N per kg of NO_3^--N) incorporates three components: (i) groundwater and surface drainage (EF_{5g}); (ii) rivers (EF_{5r}); (iii) and estuaries (EF_{5e}). In the last IPPC report (2019), the EF_{5r} and EF_{5e} were adapted to 0.26 according to 91 data observations compiled by (Tian et al., 2019), and a mean value of the EF_{5g} for ground and surface drainage was 0.60.

N_2O emissions can be influence by several factors, yet to avoid adding up uncertainties we applied the constant ratios (Table 2) proposed for freshwater wetlands, for flooded soils and by the IPCC applied by Guilhen et al., 2020 on the Amazon Basin.

The previously explained functions are the structure of the WSDM, the variables acronyms, units and description are summarised in Table 1, likewise for constants presented in Table 2.

Table 1. Variables for Wetlands Soil Denitrification Model.

Variable	Units	Description
φ	-	Porosity
ρ_b	kg·dm^{-3}	Dry sediment density
T_i	°C	Temperature
SM_i	m^3·m^{-3}	Soil saturation
SM_{res}	m^3·m^{-3}	Minimal soil saturation capacity
SM_{sat}	m^3·m^{-3}	Maximal soil saturation capacity
$[OrgC]$	mole kg^{-1}	Organic carbon content
C_{org}	gC·kg^{-1}	Organic carbon content
$[NO_{3\,i}^{-}]$	mgN.kg^{-1}	Nitrates concentration
$[NO_{3\,i}^{-}]_{nit}$	mgN.kg^{-1}	Nitrates in soil
$[NO_{3\,i}^{-}]_{denit}$	mgN.kg^{-1}	Nitrates denitrified
MAT	°C	Mean annual temperature
$C:N$	-	C: N ratio

N_{org}	mgN.kg^{-1}	Organic nitrogen

Table 2. Constants for Wetlands Soil Denitrification Model.

Constant	Value	Units	Description	Reference
T_{opt}	25	°C	Optimal temperature	Billen et al., 2018
$soil_{act}$	30	cm	Soil active layer depth	Yang et al., 2019
$k_{NO_3^-}$	0.18	mgN.kg^{-1}	Nitrate limitation constant	This study
Freshwater Marsh k_{oc}	0.062	day	Mineralization rate	Yin et al., 2019
Flooded forest k_{oc}	0.016			Bridgham et al., 1998
Freshwater wetlands R_{N2O}	0.02	-	Emission ratio	Scheer et al., 2020
Flooded soils R_{N2O}	0.082			Schlesinger, 2009
IPPC generic R_{N2O}	0.1			Guilhen et al., 2020

3.2 Wetlands Soils Denitrification Model Validation

The Amazon basin was selected as it is considered to have the optimal denitrification conditions, with a mean annual temperature of 26.6°C with little variations; average rainfall is 2100 mm per year (Ribeiro and Adis, 1984). Amazonian floodplains are directly linked to the lateral flood pulses (Junk et al., 1989; Keizer et al., 2014). It has a very regular annual bimodal flood pulse that defines a zonation along the flooding gradient of the central amazon floodplains (Kubitzki, 1989). The Amazon river discharges roughly fifteen to twenty percent of the world's annual continental freshwater into the ocean (Pekárová et al., 2003), and Amazonian floodplain forests cover an area of more than 97,000 km^2 (Hamilton et al., 2002). Dimensions of this basin reflects the meaning of water movement and abundance in life shaping global biogeochemical cycles (Vörösmarty et al., 1989).

To calibrate $k_{NO_3^-}$ and validate the WSDM, a field campaign in the central Amazonian floodplain (from 14th to 24th February 2020) was carried out to collect soil samples at eight sampling sites. The sampling points were distributed on the three main tributaries (Negro river, Solimões river and Madeira river) with different water quality. In each river, the two main wetland typologies (i.e. Freshwater marsh and Flooded forest) were sampled as shown in Figure 2.

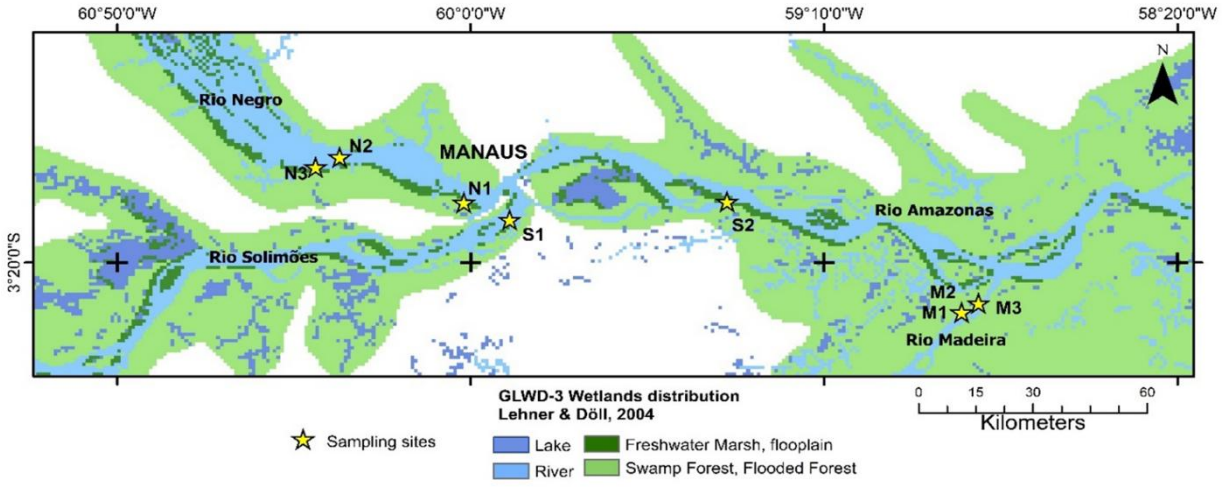

Figure 2. Sampling sites distributed in the central Amazonian floodplain, Negro river (N1, N2, N3), Solimões river (S1, S2, S3), Madeira river (M1, M2, M3). The sampling points are distributed in two main non-permanent wetland types: floodplain (light green) and flooded forest (dark green). Wetlands classification from Lehner and Doll, (2004).

The model validation was carried out in three steps: (a) *static denitrification validation*, comparing modelled potential denitrification and experimental denitrifier enzyme activity (hereafter DEA) results. DEA was measured using acetylene-inhibition technique (AIT) as described and applied in several studies (Balderston et al., 1976; Koschorreck and Darwich, 2003; Tiedje et al., 1984,Tiedje et al., 1989) detailed methodology applied in this study is presented in Appendix - Experimental Methodology. (b) *dynamic denitrification validation*, nitrates soil budget and denitrification events were modelled using soil moisture and temperature diurnal satellite input data from (2011-2019), extracted at the eight sampling points WSDM results of the eight sample sites annual denitrification rates are presented on the Appendix Table A.4. (c) *N_2O-N_2 ratio validation*, R_{N2O} = 0.02 proposed for freshwater wetlands ecosystems by Scheer et al., (2020) was applied to yearly denitrification WSDM values for each soil sample (Appendix Table A.5). N_2O range emission was calculated for freshwater wetlands and compared with other studies in order to validate the WSDM total denitrification assessment (Appendix Table A.2).

4. Results

4.1 Static Denitrification validation

To illustrate the performance of the WSDM and the behaviour regarding the three main physical parameters, three soil samples results, each from three different effluents (Negro river -N1, Solimões river- S2, Madeira river- M2), are presented in the following figures. Figure 3a. shows the soil saturation gradient, Figure 3b, the temperature gradient with 25°C as the optimal temperature and 4°C, as the activation temperature, and Figure 3c shows the soil nitrate pool. Complete modelled results for each sampling soil are compared to observed denitrification rates in laboratory-controlled conditions (Appendix Table A.2). The observations and model outputs have a good fit (*p-value* < 0.001) PBIAS = 4.15 where PBIAS is the percent bias between model and observation (Yapo et al., 1996), DEA and model maximal denitrification have a Pearson coefficient of 0.68 with a *p-value* = 0.05.

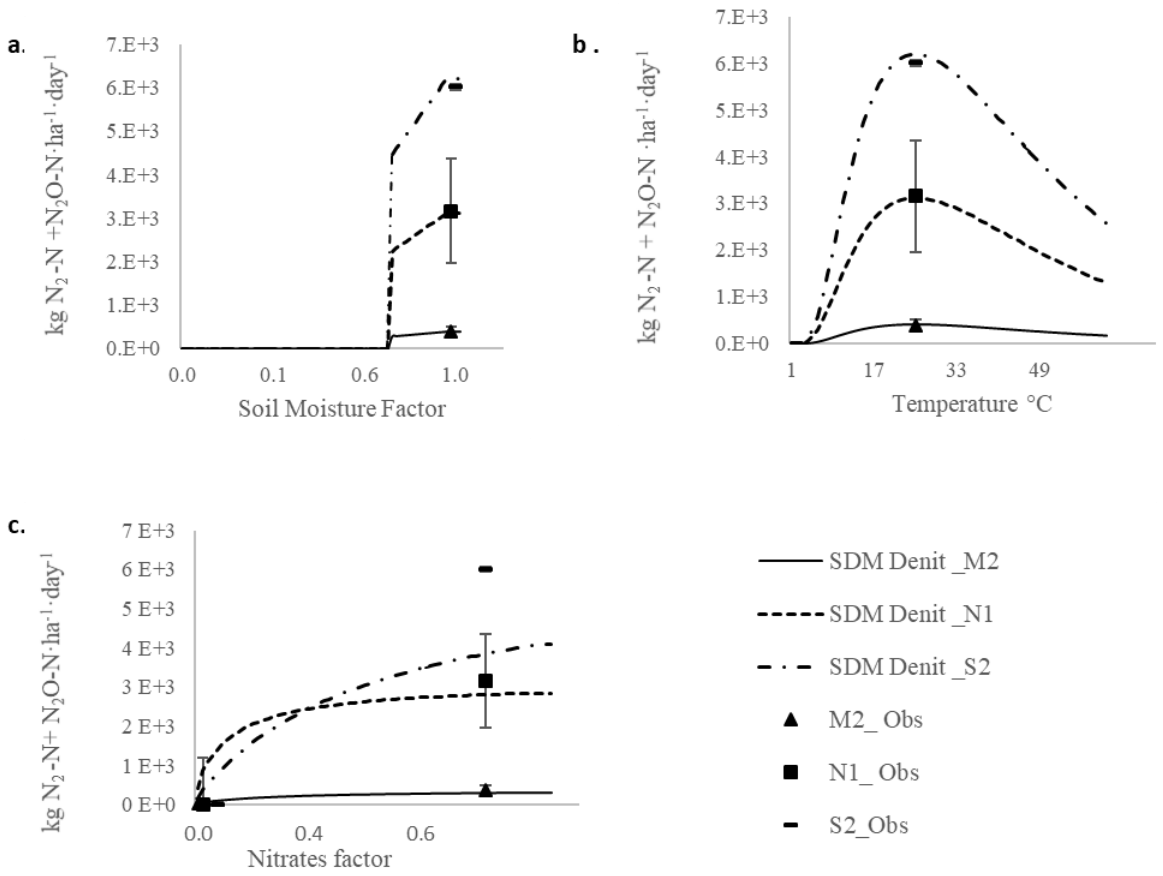

Figure 3. Model responses to different limiting factors (**a.** soil moisture, **b**. temperature, **c**. nitrate concentration) of three sample sites (Madeira river (M2), Negro river (N1), and Solimões river (S2), compared to DEA laboratory mean observations (n=3).

4.2 Dynamic Denitrification validation

Three sampling points (Negro river - N1, Solimões river - S2, Madeira river - M2) are shown as an example (Figure 4a-c). These time series show that each sampling points have different soil moisture dynamics. For instance, M2, the sampling point influenced by Madeira river (Figure 4.b) has an annual bimodal inundation dynamic, with one important denitrification event per year. When soil moisture is very low, nitrification becomes inactive and the nitrates soil budget of the soil stays constant. Low soil moisture events are present in 2012, 2015 and 2016 in the three wetland areas influenced by the three rivers. When the flooding of the plains begins, the nitrate budget is rapidly consumed. In the case of the Negro river - N1 and Solimões river - S2, soil saturation events are more frequent, so the nitrates budget is consumed faster and there are more denitrification events per year.

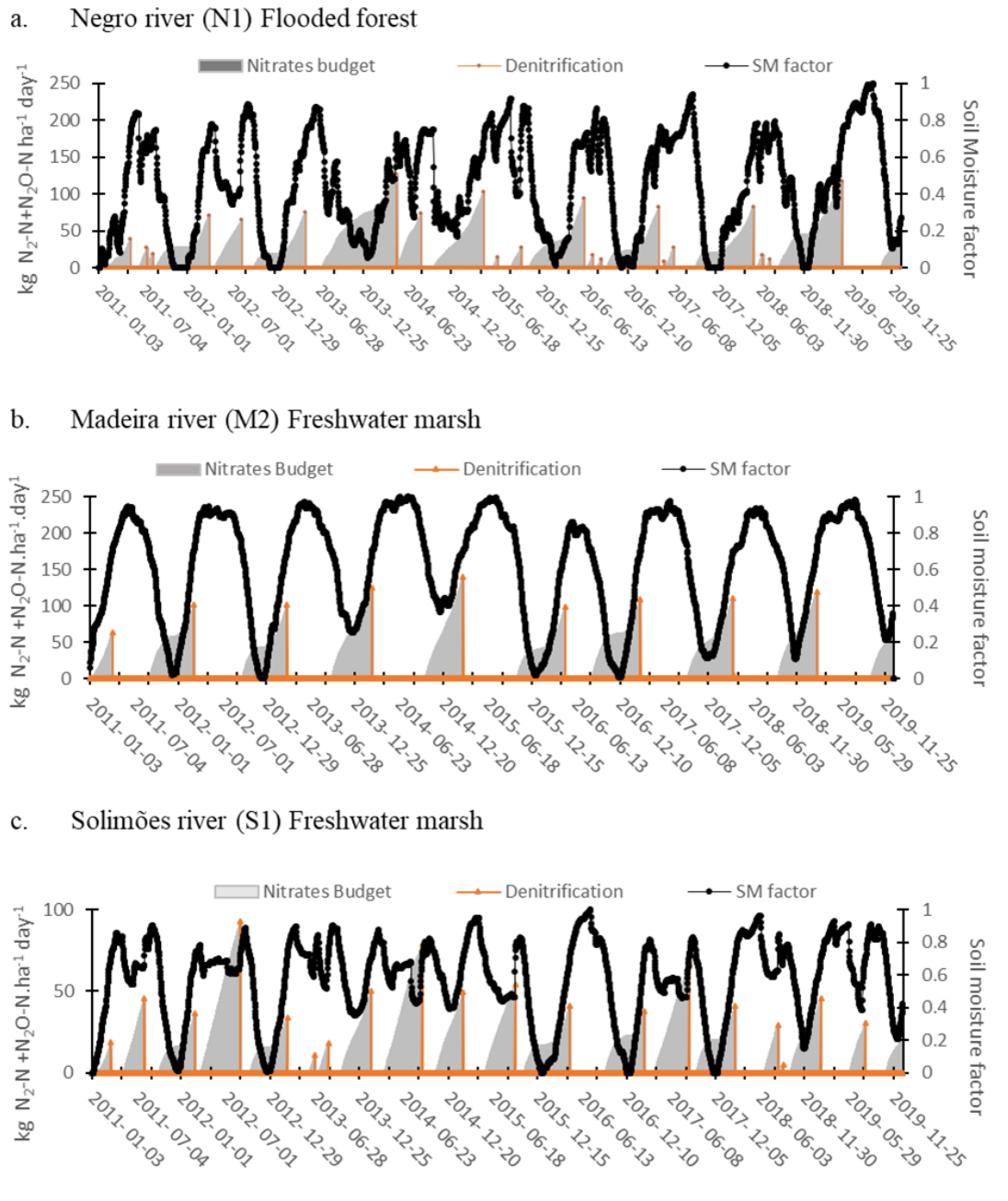

Figure 4 a-c. Diurnal time series from 2011-2019, on the main y-axis, nitrate budget per day (kgN.ha^{-1}.day^{-1}) and total denitrification (N_2+N_2O) (kgN.ha^{-1}.day^{-1}) are represented, while daily soil moisture factor dynamics are represented. The nitrate budget represents the nitrates available in the soil on a certain date, this budget is not produced in one day by nitrification, but is the accumulation of several days, therefore is represented as an area, that is consumed by denitrification events (orange lines). When soil moisture factor is zero (black line), there is no nitrification and therefore the nitrates budget stays steady.

4.3 N_2O-N_2 RATIO VALIDATION

The modelled annual denitrifications from 2012-2019 calculated in each sample site are grouped by wetland typology. The resulted emissions after applying the three different R_{N2O} from literature are compared with other studies in order to validate the WSDM total

347 denitrification assessment (Table 3). Yearly WSDM denitrification results for each soil
348 sample are presented in Appendix Table A.5.

349 **Table 3.** Annual N_2O-N emissions with different emission ratio for freshwater wetlands and flooded soils

Land cover, (R_{N2O})	**Denitrification Rate (kgN_2O-N ha^{-1} yr^{-1}) Mean value (range)**	**Reference**
Amazonian Forest	1.9	(Melillo et al., 2001)
Palm swamp peat	0.5 to 2.6	(van Lent et al., 2015)
Pantanal soil (day)	1.1-2.7	(Liengaard et al., 2014)
High input cropping	2.3	Peruvian Amazon (Palm et al., 2002)
Low input cropping	1.2	
Shifting cultivation fallow	0.8	
Multistrata agroforestry	0.5	
Peach palm plantation	0.8	
Forest fallow control	0.8	
Freshwater marshes, (0.02)	0.95 (0.4-1.8)	This study
Flooded forests, (0.02)	3.8 (2.3-6.3)	
Freshwater marshes, (0.082)	3.8 (1.7-7.4)	
Flooded forests, (0.082)	15.5 (9.3-25.9)	
Freshwater marshes, (0.1)	4.6 (2.0-9.0)	
Flooded forests, (0.1)	18.9 (11.4-31.6)	
Land cover	**Range (kgN_2O-N ha^{-1} yr^{-1})**	**Reference**
Amazonian Forest	1.4 - 24	(Davidson et al., 2001)
Amazonian Forest	0.38-16.2	(Meurer et al., 2016)
Freshwater marshes range	0.4 - 9.0	This study
Flooded forests range	2.3 - 31.6	

350 # 5 Discussion

351 ## 5.1 Model performance with respect to field data

352 The eight soil samples analysed are heterogeneous with soil properties ranging from low
353 organic carbon content (mineral soils) to rich organic soils. Even though the study area is
354 small compared with the Amazon watershed dimension, the freshwater marshes and flooded
355 forests, (the main freshwater wetland typologies of this basin), were sampled in each of the
356 three main tributaries (i.e. Negro, Solimões and Madeira rivers). This study is not intended to
357 better understand denitrification in the Amazon, but to use Amazon soils, as examples of
358 freshwater wetlands (flooded forest and freshwater marshes) under conditions of low
359 anthropogenic impact, with a bimodal hydrological cycle.
360 These samples were key to calibrate the WSDM and were intended to model complete
361 denitrification rates on a large scale considering wetlands heterogeneity (i.e. soil
362 characteristics and wetland typology) as well as physical dynamics (i.e. temperature and soil
363 moisture).

WSDM is built up in a binary assumption, which does not allow nitrification to happen at the same time as denitrification in the same point. Fixing a soil moisture threshold. This may not be true when looking at the microscale, as the soil structure and the root zone has some oxygen available most of the time. During wet periods, the anoxic conditions trigger three different processes: denitrification, dissimilatory nitrate reduction (DNRA) and Anammox. The WSDM, in its current configuration, does not simulate these two processes, and considers denitrification as the main path in wetlands, this assumption is endorsed by previous studies (Adame et al., 2019).

Due to the lack of *in situ* data of N_2O emission in the selected area of interest, experiments were carried out in controlled conditions (optimal temperature and saturation) allowing bacterial activity to be isolated and quantify nitrate consumption exclusively. This experimentation was key for the calibration and validation of the WSDM. Simulated denitrification has a good fit (PBIAS: 4.15) compared with denitrification values observed in controlled laboratory conditions (i.e. optimal temperature, saturated soil and limited nitrates) (Appendix Table A.2).

Flooded forest samples influenced by Negro river (N1, N3) have high organic carbon content, yet the recorded emissions are unlike. The difference lies in the concentration of nitrates in the soil. When there is nitrates surplus in soils the enzyme (*nosZ*) in charge of converting the N_2O to N_2 (the last step of denitrification) is withdrawn (Glass and Silverstein, 1999). This withdrawal is frequently observed in agricultural fields, where fertilizers are added and the type of irrigation used is flooding (Burgin and Groffman, 2012; Liu and Greaver, 2009).

Flooded forest soil sample (N1) influenced by the Negro river located downstream of the city of Manaus recorded a N_2O emission rate of 0.32 ± 0.1 $gN.kg^{-1}.h^{-1}$, which is two times higher than four of the other soil samples (N3, S1, M1 and M2). These four sites register a ratio that favours N_2. On the other hand, flooded forest (N3), registered the highest N_2 emission rate (0.23 ± 0.02 g N kg^{-1} h^{-1}).

N1 and N3 samples are examples of high potential denitrification rates of Amazonian wetlands soils. Extensive fertilizer use in this watershed will have a negative effect in wetlands denitrification, as concentration of nitrates from exogenous sources will increase the budget of nitrates produced by nitrification, that in turn will increase denitrification event intensity (fold-4) and N_2O emissions (Weier et al., 1993;Blackmer and Bremner, 1978; Pärn et al., 2021). A surplus of nitrates also affects ecosystem functionality, promotes eutrophication and biodiversity may be threatened (Huang et al., 2017; Smith, 2003).

Despite the importance of quantifying anthropogenic influence in natural wetlands, this version of the WSDM does not aim to calculate denitrification rates of anthropogenic input effects, but to identify physical parameters that shape the denitrification capacity of each wetland ecosystem, and assess these dynamics.

The major contribution of WSDM, is that simulated denitrification is influenced by wetland vegetation typology. The influence of the vegetation in wetlands has been reported previously by Alldred and Baines, (2016), they calculated that the presence of plants increased denitrification rates by 55% on average, but they also acknowledge the need to differentiate plant communities. The WSDM modelled these two factors, including a wetland typology that

assumes a classification of wetlands ecosystems based on their vegetation structure (i.e. trees or herbs).

The link between vegetation and bacterial processes such as denitrification can be delicate. The interaction occurs in the root areas, on a very local scale and depends on many physical and chemical aspects. Denitrification emission ratio depends on many local variables and it can exhibit drastic changes (i.e. pH, nitrate concentration). Acetylene-inhibition technique (AIT) has limitations regarding the N_2O:N_2 emission ratio, and it has been shown to be inaccurate when recording low denitrification rates such as in groundwater. Nevertheless, AIT allows an estimation of total denitrification at high temporal resolution and on small spatial scales, with limited workload and costs involved (Felber et al., 2012). A stable isotope approach might have been a preferable method to identify N_2 emissions. However, we had reservations concerning detection limits and how well the enriched solution would be distributed through the soil column.

Therefore, in the case of the WSDM the optimal compromise between accuracy and the available information was to link wetland typology to carbon decomposition rate (k_{OC}). This immediately implies the presence of bacterial community activity and integrates the different kinds of organic matter available. This correlation was validated with the denitrification rates observed in laboratory analysis, confirming that flooded forest samples had higher denitrification rates than freshwater marshes (both in optimal conditions).

5.2 Comparison with earlier modelling approaches

The precedent denitrification model estimates a total denitrification (N_2-N + N_2O-N) rates at the Amazon floodplains from 38.8 to 142.5 kgN.ha^{-1}.yr^{-1} with a spatial grid of 25 km^2 (Guilhen et al., 2020). The WSDM has a wider range (20.36 - 315.90 kgN.ha^{-1}.yr^{-1}), this difference is a consequence of model set up, the current version is sensitive to different organic carbon decomposition rates, soil moisture gradient, as well as nitrates limitation, calculated in 1 km^2 grid, constraints that were missing in the previous version.

The WSDM assumed that annual input flux of carbon is greater than losses (respiration; harvesting, export, burial). Consequently, carbon budget is set constant but not unlimited. Other studies had modelled variable carbon input (Fabre et al., 2020; Guilhen et al., 2020; Peyrard et al., 2011) showing that carbon is not a limiting factor but it can enhance the denitrification signal. This assumption is compensated by the mineralization rate of organic carbon (K_{OC}), which is specific for each kind of simplified wetland ecosystem typology.

The WSDM current version does not calculates N_2O:N_2 ratio yet. The different N_2O rate productions (Table 3), suggest that ratio (0.02) for freshwater wetlands proposed by Scheer et al., (2020) applied to the WSDM denitrification results, gives a N_2O-N total contribution within the range of what has been reported in low impacted Amazonian soils by other studies. This estimation should be taken as an indicator and could be improved by field measurements with other methodologies as ^{15}N isotopic tracers (Bergsma et al., 2001). Additionally, Pärn et al., (2021) reported by *in situ* measurements that the Peruvian palm peat swamp is a hot spot and that the emission ratio change depending on the season. They reported that March (the main peak) has low N_2O emissions, and very high N_2 potential. On the other hand, in

September the emission rate has a higher N_2O production ratio. The same pattern was observed in the modelled time series, regarding the activation of denitrification, however the WSDM in the current version does not calculate seasonal N_2O:N_2 ratios, but this evidence could serve for developing a N_2O:N_2 ratio function.

Relevant research has been done on this topic, on a large scale the Global N_2O Model Intercomparison Project (Tian et al., 2018) presented a spatialized global-scale N_2O estimate by making a comparative study of a dozen of hydrodynamic models that model the global nitrogen and carbon cycles. The resulted model, the Dynamic Land Ecosystem Model (DLEM), assesses the pre-industrial emissions (CO_2, CH_4 and N_2O) and the current trend, on a yearly, monthly and daily basis from 1901 to 2010 with a spatial resolution of 0.5° × 0.5°. This model exposes the anthropogenic impact, main pollution sources and the consequences towards the biosphere. This model also takes into account different ecosystems and divides wetlands into four categories (seasonal grass wetlands, seasonal forest wetlands, permanent grass wetlands and permanent forest wetlands).

Likewise, DNDC (DeNitrification DeComposition) model is a powerful tool to evaluate N_2O production, consumption and transport in agricultural soils, it was later modified and adapted to other ecosystems. Wetland-DNDC (Gilhespy et al., 2014) was adapted to calculate carbon emissions (CO_2 and CH_4). These two models have been improved by the scientific community for several years, and they are currently a very robust approach to local GHG emissions, and water dynamics. Both models have an empirical base that operate at watershed scale and demand copious input datasets, that may not be available for several tropical wetlands.

WSDM, is complementary to both models, takes into account different wetlands ecosystems based on the vegetation structure, but with a simplified approach that is useful at large scale. The results are given in terms of total denitrification, aiming to contribute with a particular vision of natural wetlands and their positive role in the global nitrogen cycle This natural wetland function via complete denitrification is often overlooked. The total denitrification account non-harmful emissions (N_2), which implies the subtraction of nitrate flux into aquatic ecosystems (i.e. rivers, lakes, coastal areas).

6 Conclusion

The WSDM main contribution is that it considers wetlands diversity, and calculates denitrification in a diurnal basis while remaining parsimonious, giving a dynamic spatialized assessment that identifies hot moments and hot spots. WSDM total denitrification can be used as an indicator tool for prioritizing conservation areas, or wetlands ecosystems that must be studied in depth. The WSDM was developed for a large-scale approach, as it does not require a watershed-based model. The main drivers of the model are soil moisture and temperature input data which have been identified as key for modelling the nitrate budget, and denitrification activation-deactivation dynamics at diurnal basis. Modelling these dynamics is a tool in wetlands areas where field data is not available yet. These results may be indicators of possible scenarios when the anomalies will repeat and/or intensify. In future, this model can be applied at different scales (continents or regions) as well as in different watersheds at different climatic regimes (i.e. boreal or temperate).

7 Acknowledgements

The research presented in this paper is funded by CONACYT (The Mexican National Council for Science and Technology) in the frame of a PhD research grant (Scholar/Scholarship reference: 625261/ 471711 2017-2021) at Université Toulouse III -Paul Sabatier, Toulouse, France. TOSCA-SOLE project from French Space agency CNES for financial support.

8 References

Adame, M.F., Franklin, H., Waltham, N.J., Rodriguez, S., Kavehei, E., Turschwell, M.P., Balcombe, S.R., Kaniewska, P., Burford, M.A., Ronan, M., 2019. Nitrogen removal by tropical floodplain wetlands through denitrification. Marine and Freshwater Research 70, 1513–1521.

Ahmad, A.B., Mahmoodi Ali, 2020. Algorithm Theoretical Basis Document (ATBD) for the SMOS Level 4 Root Zone Soil Moisture. Zenodo. https://doi.org/10.5281/ZENODO.4298572

Al Bitar, A., Mialon, A., Kerr, Y.H., Cabot, F., Richaume, P., Jacquette, E., Quesney, A., Mahmoodi, A., Tarot, S., Parrens, M., 2017. The global SMOS Level 3 daily soil moisture and brightness temperature maps. Earth System Science Data 9, 293.

Alldred, M., Baines, S.B., 2016. Effects of wetland plants on denitrification rates: a meta-analysis. Ecol Appl 26, 676–685. https://doi.org/10.1890/14-1525

Asaeda, T., Trung, V.K., Manatunge, J., 2000. Modeling the effects of macrophyte growth and decomposition on the nutrient budget in Shallow Lakes. Aquatic Botany 68, 217–237. https://doi.org/10.1016/S0304-3770(00)00123-6

Asaeda, T., Van Bon, T., 1997. Modelling the effects of macrophytes on algal blooming in eutrophic shallow lakes. Ecological Modelling 104, 261–287. https://doi.org/10.1016/S0304-3800(97)00129-4

Bakken, L.R., Bergaust, L., Liu, B., Frostegård, Å., 2012. Regulation of denitrification at the cellular level: a clue to the understanding of N2O emissions from soils. Philosophical Transactions of the Royal Society B: Biological Sciences 367, 1226–1234.

Balderston, W.L., Sherr, B., Payne, W.J., 1976. Blockage by acetylene of nitrous oxide reduction in Pseudomonas perfectomarinus. Applied and Environmental Microbiology 31, 504–508.

Bateman, E.J., Baggs, E.M., 2005. Contributions of nitrification and denitrification to N2O emissions from soils at different water-filled pore space. Biol Fertil Soils 41, 379–388. https://doi.org/10.1007/s00374-005-0858-3

Batjes, N.H., 2015. World soil property estimates for broad-scale modelling (WISE30sec). ISRIC - World Soil Information, Wageningen.

Bergsma, T.T., Ostrom, N.E., Emmons, M., Robertson, G.P., 2001. Measuring simultaneous fluxes from soil of N2O and N2 in the field using the 15N-gas “nonequilibrium” technique. Environmental science & technology 35, 4307–4312.

Berner, R.A., 1980. Early diagenesis: a theoretical approach. Princeton University Press.

Billen, G., Ramarson, A., Thieu, V., Théry, S., Silvestre, M., Pasquier, C., Hénault, C., Garnier, J., 2018. Nitrate retention at the river–watershed interface: a new conceptual modeling approach. Biogeochemistry 139, 31–51.

Blackmer, A.M., Bremner, J.M., 1978. Inhibitory effect of nitrate on reduction of N2O to N2 by soil microorganisms. Soil Biology and Biochemistry 10, 187–191. https://doi.org/10.1016/0038-0717(78)90095-0

Boyer, E.W., Alexander, R.B., Parton, W.J., Li, C., Butterbach-Bahl, K., Donner, S.D., Skaggs, R.W., Del Grosso, S.J., 2006. Modeling denitrification in terrestrial and aquatic ecosystems at regional scales. Ecological Applications 16, 2123–2142.

Bridgham, S.D., Updegraff, K., Pastor, J., 1998. Carbon, nitrogen, and phosphorus mineralization in northern wetlands. Ecology 79, 1545–1561.

Burgin, A.J., Groffman, P.M., 2012. Soil O2 controls denitrification rates and N2O yield in a riparian wetland. J Geophys Res 117.
Canfield, D.E., Glazer, A.N., Falkowski, P.G., 2010. The Evolution and Future of Earth's Nitrogen Cycle. Science 330, 192–196. https://doi.org/10.1126/science.1186120
Chen, H., Mothapo, N.V., Shi, W., 2015. Soil Moisture and pH Control Relative Contributions of Fungi and Bacteria to N2O Production. Microb Ecol 69, 180–191. https://doi.org/10.1007/s00248-014-0488-0
Ciais, P., Sabine, C., Bala, G., Bopp, L., Brovkin, V., Canadell, J., Chhabra, A., DeFries, R., Galloway, J., Heimann, M., 2014. Carbon and other biogeochemical cycles, in: Climate Change 2013: The Physical Science Basis. Contribution of Working Group I to the Fifth Assessment Report of the Intergovernmental Panel on Climate Change. Cambridge University Press, pp. 465–570.
Davidson, E.A., Bustamante, M.M.C., de Siqueira Pinto, A., 2001. Emissions of Nitrous Oxide and Nitric Oxide from Soils of Native and Exotic Ecosystems of the Amazon and Cerrado Regions of Brazil. TheScientificWorldJOURNAL 1, 312–319. https://doi.org/10.1100/tsw.2001.261
Fabre, C., Sauvage, S., Guilhen, J., Cakir, R., Gerino, M., Sánchez-Pérez, J.M., 2020. Daily denitrification rates in floodplains under contrasting pedo-climatic and anthropogenic contexts: modelling at the watershed scale. Biogeochemistry. https://doi.org/10.1007/s10533-020-00677-4
Felber, R., Conen, F., Flechard, C.R., Neftel, A., 2012. Theoretical and practical limitations of the acetylene inhibition technique to determine total denitrification losses. Biogeosciences 9, 4125–4138.
Gilhespy, S.L., Anthony, S., Cardenas, L., Chadwick, D., del Prado, A., Li, C., Misselbrook, T., Rees, R.M., Salas, W., Sanz-Cobena, A., 2014. First 20 years of DNDC (DeNitrification DeComposition): model evolution. Ecological modelling 292, 51–62.
Girard, M.-C., Walter, C., Rémy, J.-C., Berthelin, J., Morel, J.-L., 2011. Sols et environnement - 2e édition - Cours, exercices et études de cas - Livre+compléments en ligne: Cours, exercices corrigés et études de cas. Dunod.
Glass, C., Silverstein, J., 1999. Denitrification of high-nitrate, high-salinity wastewater. Water Research 33, 223–229. https://doi.org/10.1016/S0043-1354(98)00177-8
Green, P.A., Vörösmarty, C.J., Meybeck, M., Galloway, J.N., Peterson, B.J., Boyer, E.W., 2004. Pre-industrial and contemporary fluxes of nitrogen through rivers: a global assessment based on typology. Biogeochemistry 68, 71–105.
Groffman, P.M., Tiedje, J.M., 1988. Denitrification hysteresis during wetting and drying cycles in soil. Soil Sci Soc Am J 52. https://doi.org/10.2136/sssaj1988.03615995005200060022x
Grosso, S.J.D., Wirth, T., Ogle, S.M., Parton, W.J., 2008. Estimating Agricultural Nitrous Oxide Emissions. Eos, Transactions American Geophysical Union 89, 529–529. https://doi.org/10.1029/2008EO510001
Guilhen, J., Al Bitar, A., Sauvage, S., Parrens, M., Martinez, J.-M., Abril, G., Moreira-Turcq, P., Sanchez-Pérez, J.-M., 2020. Denitrification, carbon and nitrogen emissions over the Amazonianwetlands (preprint). Biogeochemistry: Wetlands. https://doi.org/10.5194/bg-2020-3
Hamilton, S.K., Sippel, S.J., Melack, J.M., 2002. Comparison of inundation patterns among major South American floodplains. Journal of Geophysical Research: Atmospheres 107, LBA 5-1-LBA 5-14.
Hénault, C., Germon, J.C., 2000. NEMIS, a predictive model of denitrification on the field scale. European Journal of Soil Science 51, 257–270.
Huang, J., Xu, C., Ridoutt, B.G., Wang, X., Ren, P., 2017. Nitrogen and phosphorus losses and eutrophication potential associated with fertilizer application to cropland in China. Journal of Cleaner Production 159, 171–179.
Hunter, K.S., Wang, Y., Van Cappellen, P., 1998. Kinetic modeling of microbially-driven redox chemistry of subsurface environments: coupling transport, microbial metabolism and

geochemistry. Journal of Hydrology 209, 53–80. https://doi.org/10.1016/S0022-1694(98)00157-7
Junk, W.J., Bayley, P.B., Sparks, R.E., 1989. The flood pulse concept in river-floodplain systems. Canadian special publication of fisheries and aquatic sciences 106, 110–127.
Keizer, F.M., Schot, P.P., Okruszko, T., Chormański, J., Kardel, I., Wassen, M.J., 2014. A new look at the Flood Pulse Concept: The (ir)relevance of the moving littoral in temperate zone rivers. Ecological Engineering 64, 85–99. https://doi.org/10.1016/j.ecoleng.2013.12.031
Koschorreck, M., Darwich, A., 2003. Nitrogen dynamics in seasonally flooded soils in the Amazon floodplain. Wetlands Ecology and Management 11, 317–330. https://doi.org/10.1023/B:WETL.0000005536.39074.72
Kubitzki, K., 1989. The ecogeographical differentiation of Amazonian inundation forests. Plant Systematics and Evolution 162, 285–304.
Lehner, B., Doll, P., 2004. Development and validation of a global database of lakes, reservoirs and wetlands. J. Hydrol. 296, 1–22. https://doi.org/10.1016/j.jhydrol.2004.03.028
Liengaard, L., Figueiredo, V., Markfoged, R., Revsbech, N.P., Nielsen, L.P., Prast, A.E., Kühl, M., 2014. Hot moments of N2O transformation and emission in tropical soils from the Pantanal and the Amazon (Brazil). Soil Biology and Biochemistry 75, 26–36. https://doi.org/10.1016/j.soilbio.2014.03.015
Liu, L., Greaver, T.L., 2009. A review of nitrogen enrichment effects on three biogenic GHGs: the CO2 sink may be largely offset by stimulated N2O and CH4 emission. Ecology letters 12, 1103–1117.
Martínez-Espinosa, C., Sauvage, S., Al Bitar, A., Green, P.A., Vörösmarty, C.J., Sánchez-Pérez, J.M., 2021. Denitrification in wetlands: A review towards a quantification at global scale. Science of The Total Environment 754, 142398. https://doi.org/10.1016/j.scitotenv.2020.142398
Melillo, J.M., Steudler, P.A., Feigl, B.J., Neill, C., Garcia, D., Piccolo, M.C., Cerri, C.C., Tian, H., 2001. Nitrous oxide emissions from forests and pastures of various ages in the Brazilian Amazon. Journal of Geophysical Research: Atmospheres 106, 34179–34188. https://doi.org/10.1029/2000JD000036
Meurer, K.H.E., Franko, U., Stange, C.F., Rosa, J.D., Madari, B.E., Jungkunst, H.F., 2016. Direct nitrous oxide (N_2O) fluxes from soils under different land use in Brazil—a critical review. Environ. Res. Lett. 11, 023001. https://doi.org/10.1088/1748-9326/11/2/023001
Palm, C.A., Alegre, J.C., Arevalo, L., Mutuo, P.K., Mosier, A.R., Coe, R., 2002. Nitrous oxide and methane fluxes in six different land use systems in the Peruvian Amazon. Global Biogeochemical Cycles 16, 21-1-21–13. https://doi.org/10.1029/2001GB001855
Pärn, J., Soosaar, K., Schindler, T., Machacova, K., Alegría Muñoz, W., Fachín, L., Jibaja Aspajo, J.L., Negron-Juarez, R.I., Maddison, M., Rengifo, J., Dinis, D.J.G., Oversluijs, A.G.A., Fucos, M.C.Á., Vásquez, R.C., Huaje Wampuch, R., Peas García, E., Sohar, K., Cordova Horna, S., Gómez, T.P., Urquiza Muñoz, J.D., Tello Espinoza, R., Mander, Ü., 2021. High greenhouse gas fluxes from peatlands under various disturbances in the Peruvian Amazon. Biogeosciences Discussions 1–13. https://doi.org/10.5194/bg-2021-46
Pasut, C., Tang, F.H.M., Hamilton, D., Riley, W.J., Maggi, F., 2021. Spatiotemporal Assessment of GHG Emissions and Nutrient Sequestration Linked to Agronutrient Runoff in Global Wetlands. Global Biogeochemical Cycles 35, e2020GB006816. https://doi.org/10.1029/2020GB006816
Pekárová, P., Miklánek, P., Pekár, J., 2003. Spatial and temporal runoff oscillation analysis of the main rivers of the world during the 19th–20th centuries. Journal of Hydrology 274, 62–79.
Peyrard, D., Delmotte, S., Sauvage, S., Namour, Ph., Gerino, M., Vervier, P., Sanchez-Perez, J.M., 2011. Longitudinal transformation of nitrogen and carbon in the hyporheic zone of an N-rich stream: A combined modelling and field study. Physics and Chemistry of the Earth, Parts A/B/C, Man and River Systems: From pressures to physical, chemical and ecological status 36, 599–611. https://doi.org/10.1016/j.pce.2011.05.003

637 Quin, A., Jaramillo, F., Destouni, G., 2015. Dissecting the ecosystem service of large-scale pollutant
638 retention: The role of wetlands and other landscape features. AMBIO 44, 127–137.
639 https://doi.org/10.1007/s13280-014-0594-8
640 Ribeiro, M. de N.G., Adis, J., 1984. Local rainfall variability-a potential bias for bioecological studies in
641 the Central Amazon. Acta Amazonica 14, 159–174.
642 Scheer, C., Fuchs, K., Pelster, D.E., Butterbach-Bahl, K., 2020. Estimating global terrestrial
643 denitrification from measured N2O:(N2O+ N2) product ratios. Current Opinion in
644 Environmental Sustainability 47, 72–80.
645 Schlesinger, W.H., 2009. On the fate of anthropogenic nitrogen. Proc. Natl. Acad. Sci. U. S. A. 106,
646 203–208. https://doi.org/10.1073/pnas.0810193105
647 Smith, V.H., 2003. Eutrophication of freshwater and coastal marine ecosystems - A global problem.
648 Environ. Sci. Pollut. Res. 10, 126–139. https://doi.org/10.1065/espr2002.12.142
649 Thorslund, J., Jarsjo, J., Jaramillo, F., Jawitz, J.W., Manzoni, S., Basu, N.B., Chalov, S.R., Cohen, M.J.,
650 Creed, I.F., Goldenberg, R., 2017. Wetlands as large-scale nature-based solutions: Status and
651 challenges for research, engineering and management. Ecological Engineering 108, 489–497.
652 Tian, H., Chen, G., Lu, C., Xu, X., Ren, W., Zhang, B., Banger, K., Tao, B., Pan, S., Liu, M., Zhang, C.,
653 Bruhwiler, L., Wofsy, S., 2015. Global methane and nitrous oxide emissions from terrestrial
654 ecosystems due to multiple environmental changes. Ecosystem Health and Sustainability 1,
655 1–20. https://doi.org/10.1890/EHS14-0015.1
656 Tian, H., Xu, R., Canadell, J.G., Thompson, R.L., Winiwarter, W., Suntharalingam, P., Davidson, E.A.,
657 Ciais, P., Jackson, R.B., Janssens-Maenhout, G., Prather, M.J., Regnier, P., Pan, N., Pan, S.,
658 Peters, G.P., Shi, H., Tubiello, F.N., Zaehle, S., Zhou, F., Arneth, A., Battaglia, G., Berthet, S.,
659 Bopp, L., Bouwman, A.F., Buitenhuis, E.T., Chang, J., Chipperfield, M.P., Dangal, S.R.S.,
660 Dlugokencky, E., Elkins, J.W., Eyre, B.D., Fu, B., Hall, B., Ito, A., Joos, F., Krummel, P.B.,
661 Landolfi, A., Laruelle, G.G., Lauerwald, R., Li, W., Lienert, S., Maavara, T., MacLeod, M., Millet,
662 D.B., Olin, S., Patra, P.K., Prinn, R.G., Raymond, P.A., Ruiz, D.J., van der Werf, G.R., Vuichard,
663 N., Wang, J., Weiss, R.F., Wells, K.C., Wilson, C., Yang, J., Yao, Y., 2020. A comprehensive
664 quantification of global nitrous oxide sources and sinks. Nature 586, 248–256.
665 https://doi.org/10.1038/s41586-020-2780-0
666 Tian, H., Yang, J., Lu, C., Xu, R., Canadell, J.G., Jackson, R., Arneth, A., Chang, J., Chen, G., Ciais, P.,
667 2018. The Global N2O Model Intercomparison Project, B. Am. Meteorol. Soc., 99, 1231–1251.
668 Tian, L., Cai, Y., Akiyama, H., 2019. A review of indirect N2O emission factors from agricultural
669 nitrogen leaching and runoff to update of the default IPCC values. Environmental pollution
670 245, 300–306.
671 Tiedje, J.M., Sexstone, A.J., Parkin, T.B., Revsbech, N.P., 1984. Anaerobic processes in soil. Plant Soil
672 76, 197–212. https://doi.org/10.1007/BF02205580
673 Tiedje, J.M., Simkins, S., Groffman, P.M., 1989. Perspectives on measurement of denitrification in the
674 field including recommended protocols for acetylene based methods. Plant Soil 115, 261–
675 284. https://doi.org/10.1007/BF02202594
676 van Lent, J., Hergoualc'h, K., Verchot, L.V., 2015. Reviews and syntheses: Soil N 2 O and NO emissions
677 from land use and land-use change in the tropics and subtropics: a meta-analysis.
678 Biogeosciences 12, 7299–7313.
679 Vörösmarty, C.J., Moore III, B., Grace, A.L., Gildea, M.P., Melillo, J.M., Peterson, B.J., Rastetter, E.B.,
680 Steudler, P.A., 1989. Continental scale models of water balance and fluvial transport: An
681 application to South America. Global biogeochemical cycles 3, 241–265.
682 Weier, K.L., Doran, J.W., Power, J.F., Walters, D.T., 1993. Denitrification and the Dinitrogen/Nitrous
683 Oxide Ratio as Affected by Soil Water, Available Carbon, and Nitrate. Soil Sci. Soc. Am. J 57,
684 66–72.
685 Yang, Y., Zhang, H., Shan, Y., Wang, J., Qian, X., Meng, T., Zhang, J., Cai, Z., 2019. Response of
686 denitrification in paddy soils with different nitrification rates to soil moisture and glucose
687 addition. Science of The Total Environment 651, 2097–2104.
688 https://doi.org/10.1016/j.scitotenv.2018.10.066

689 Yapo, P.O., Gupta, H.V., Sorooshian, S., 1996. Automatic calibration of conceptual rainfall-runoff
690 models: sensitivity to calibration data. Journal of hydrology 181, 23–48.
691 Yin, S., Bai, J., Wang, W., Zhang, G., Jia, J., Cui, B., Liu, X., 2019. Effects of soil moisture on carbon
692 mineralization in floodplain wetlands with different flooding frequencies. Journal of
693 Hydrology 574, 1074–1084. https://doi.org/10.1016/j.jhydrol.2019.05.007

694
695

Appendix

Experimental methodology

Soil samples of each site were collected, conserved at 4 °C, transported to Toulouse, France for further analysis. Sixty grams of each soil type were divided into three 125 ml glass flasks, having ~ 20 g per flask (n=3 each soil type). Biological activity was re-established in stored soils by incubating 48 hours at 25°C and 20 ml of deoxygenated water was added, having a saturated water-filled pore space. Each container was sealed with a screw-up lid in which a septum had been fitted for gas sampling. Weight of the glass flasks before, and after adding the soil sample and water were taken. The gas chromatograph was used in parallel with the G200 N_2O device for quantifying N_2O emission from soil activity in the control records as emissions were low. For the potential denitrification concentrations recorded were within the recording range of the real-time device (G200) (>1 ppm), therefore, it was used as the only reading device for the rest of the experiments. To achieve potential denitrification rates, soil cores were incubated during three hours at 25°C, under anaerobic condition, replacing the headspace with helium (He), 20 ml of acetylene (C_2H_2) was added to each flask at the beginning of incubation. To identify the nitrate soil saturation linked to potential denitrification, five different treatments with progression of nutrient solutions (CH_3 COOH and KNO_3) were applied.

Concentrations are shown in Table A.1 and were applied from 1 to 5. The measurement principle of total denitrification (the sum of N_2O + N_2 fluxes), in AIT treated soil samples, assumes that every N_2 molecule produced from completed denitrification which would normally be emitted from the soil system, remains in the form of N_2O, which is detected in our laboratory set-up by gas chromatography. A N_2O content of the headspace was determined every half an hour within the following three hours. Soil characteristics (NO_3^- content, Org Carbon content, bulk density, porosity) and the mean values (n=3) for each soil sample were done, are reported in Table A.2.

Table A.1 Concentration of nitrates and carbon solution applied for DEA identification.

Treatment	Vol added (ml)		Nitrogen Solution	Carbon Solution	mg N	mg C
	N	C	(mg/L)	(mg/L)		
1	5	0	100	100	0.5	0
2	5	10	100	100	0.5	1
3	0.2		10000	10000	2	2
4	0.5		10000	10000	5	5
5	1		10000	10000	10	10

Between treatments, soil samples were left for 24 hours in aerated conditions before applying the next treatment. Once all the treatments were completed, the flasks were dried out in an oven at 100 °C for 24h. After that, the weight of each flask was measured. The dry samples were sieved and two grams of these homogenized samples were ignited at 500°C for 24h to obtain the organic matter content by weight difference. Pore space and bulk density were determined gravimetrically on volume samples assuming a measured particle density of 2.613 g cm^{-3}. Potential denitrification rates were calculated from the linear increase of the N_2O

content in the flask and expressed as µg N_2O $g^{-1}.h^{-1}$. All data is expressed per gram of sediment on a dry basis. The total N_2O production (Eq. 1) was calculated by the N_2O gas (g) fraction and N_2O liquid (l) fraction measured in ppm as follows,

$$N_2O_t = N_2O_g + N_2O_l \quad \text{Eq. 1}$$

and then converted to µg N_2O gas (Eq.2) and liquid (Eq. 3) as follows,

$$N_2O_g = \frac{\left(2{,}211 \cdot 10^{-8} \cdot M_{ppm}\right) - (4{,}35 \cdot 10^{-9})}{\frac{0{,}00468}{1{,}817 * 10^{-3}}} \cdot 1000 \quad \text{Eq. 2}$$

$$N_2O_l = (1{,}536 * 10^{-9}) \cdot M_{ppmv} \cdot W_v \cdot 10^6 \quad \text{Eq. 3}$$

where M_{ppm} is a density fraction is expressed in part per million of air (ppm) and M_{ppmv} refers to part per million in volume of solution (ppmv; 1 ppmv = 1 µL/L), W_v water volume was calculated with the difference between the dry sample and wet sample weight.

The N-N_2O (Eq. 4), N- N_2O+N_2 (Eq. 5) and N-N_2O (Eq. 6) production ratio were calculated in dry sediment basis as follows,

$$k_{N-N_2O} = \frac{N_2O_t}{Ds} * \frac{28}{44} \quad \text{Eq. 4}$$

If C_2H_2 added, Eq. 5

$$k_{N-N_2O+N_2} = \frac{N_2O_t}{Ds} * \frac{28}{44}$$

$$k_{N-N_2} = k_{N-N_2O+N_2} - k_{N-N_2O} \quad \text{Eq. 6}$$

where k_{N-N_2O} refers to the production rate of N_2O (µg N g^{-1} h^{-1}) when there is no inhibition with acetylene, and Ds is the dry soil weight (g), when acetylene is applied then the N_2O ratio recorded is $k_{N-N_2O+N_2}$ which is the sum of (N_2 and N_2O) and is also expressed in µg N g^{-1} h^{-1}, then k_{N-N_2} refers only to the N_2 production ratio (µg N g^{-1} h^{-1}), as subtraction of the two previous equations.

744 # Results

745 ## Static validation

Table A.2. Denitrification rates from the Amazon central floodplain wetlands soil samples (laboratory-controlled conditions) and modelled with WSDM

Organic Carbon [NOC] (g.kg^{-1})	Porosity [OrgC] (g.kg^{-1})	C/N ratio K_{OC} (L.kg^{-1})	$k_{NO_3^-}$ (µmolN.kg^{-1}.d^{-1})	k_{NO} (µg N_2-N + N_2O-N.kg^{-1}.d^{-1})
190.28	0.85	16.17	9770.44	4797.77
9.45	190.28	0.006	2.46	158.64
17.13	10.49	15.43	0.003	7.50
0.04	0.18	0.122	0	188.86
89.16	9.71	11.08	0.006	10355.91
0.05	17.14	0.068	4.54	1747.30
6.70	89.16	10.34	3.3	1393.15
4.06	6.70	9.909	0.003	1747.30
12.13	0.52	9.271	2.52	3966.25
12.68	4.42	7.44	0.002	9744.47
0.19	0.59	0.004	10.18	189.97
0.64	12.66	4.52	0.067	377.42
0.06	0.39	0.264	3.64	1188.50
	0.64		0.003	1380.42
			2.31	

Table A.3. Soil samples properties and parameters used for c

749 ## Dynamic validation results

tion annual

Table A.5. Summary of N_2O-N emissions at daily and yearly basis at observed and modelled denitrification

kg N_2-N + N_2O-N ha⁻¹ day⁻¹ nitrification	R_{N2O}	interannual rate 2012-201 R_{N2O}[3]	Model ini mean nitr kg N ha
2.46	31(0.12)[1]	12(0.082)	128
N.ha⁻¹.yr⁻¹ 0	258.25	kg N_2O-N.ha⁻¹.yr⁻¹	128
4.54	1069(0.22) / 12.8	209.1 / 10.5	198
	2.6	2.1	
3.3	1441.29 / 19.2	436.1 / 14.3	315
	31.6	25.9	
6.52	6211.43 / 9.0	92.77 / 7.4	90
10.18	10648.62 / 4.9	60.62 / 4.0	49
	11.4	9.3	
3.64	389.93 / 2.0	139.89 / 1.7	114
2.31	1480.55	25.12	20

750
751 * 2011 w... led, as it is the first year of the model and the nitrate pool is building up, the me...

num rate (day⁻¹) R_{N2O}[3]	kg C	R_{N2O}	2011-20
(0.082)	90.28	(0.02)	27.46
⁻¹.day⁻¹	0.18		27.57
0.85	17.14	0.21	27.59
0.01		0.00	
2.99	89.16	0.80	27.76
0.69		0.19	
1.56	6.37	0.42	27.71
1.99	4.42	0.53	28.19
2.12		0.57	
0.41	12.66	0.11	28.19
	0.64		28.21

mary of observed and modelled denitrification.